RNA–Protein Interactions and Secondary Structures of Cowpea Chlorotic Mottle Virus for in Vitro Assembly†

B. J. M. Verduin, B. Prescott, and G. J. Thomas, Jr.*

ABSTRACT: Laser Raman spectroscopy of the cowpea chlorotic mottle virus (CCMV) in native (pH 5.0) and partially swollen (pH 7.5) states reveals the presence of small percentages of protonated adenine (<15%) and cytosine (<7%) bases in the encapsidated RNA molecule of the native virion. The protonated bases are titrated with pH-induced swelling of the virus. Titration of putative COOH groups of aspartic and glutamic side chains of the virion subunit cannot be detected over the same pH range, which suggests that carboxyl anions (CO_2^-) and protonated bases are both available at pH 5 to stabilize the ribonucleoprotein particles by electrostatic interactions. The highly (95%) ordered secondary structure of encapsidated RNA may undergo a small additional increase (<3%) in ordered structure with release from the virion, suggesting at most a marginal structure-distorting influence from protein contacts in the native particle. The Raman spectra of the virion are also compared by difference spectroscopy with spectra of capsids (empty shells devoid of RNA), subunit dimers, and protein-free RNA. The results indicate that the subunit structure is altered by the release of RNA from the virion, as well as by the swelling of the virion. Amino acid residues and protein secondary structures that are affected in these in vitro assembly and disassembly processes are identified from their characteristic Raman lines. Two classes of cysteinyl SH groups, solvent exposed and solvent protected, are revealed for the capsid and virion subunit. Shielding of SH is reduced in the subunit dimer and eliminated in core-protein dimer, the latter obtained by tryptic digestion of subunit dimers. The subunit is richest in β-sheet secondary structure for all assembly states examined.

Cowpea chlorotic mottle virus (CCMV) is an icosahedral RNA virus and a member of the bromovirus group (Bancroft, 1970; Lane, 1974). The bromoviruses are generally characterized by a multicomponent RNA genome and have been extensively studied for their ability to undergo structural transitions in vitro as a function of solution pH and ionic strength (Kaper, 1975). The virion of CCMV is a mixture of three nonidentical ribonucleoprotein particles, distinguished by slightly different buoyant densities in a CsCl gradient. The heaviest particle contains the largest RNA molecule, designated RNA-1; the particle of intermediate density contains the two smallest RNA molecules, RNA-3 and RNA-4; and the lightest particle contains RNA-2. So far as is known, all particles contain the same symmetry, with 180 identical subunits arranged in a $T = 3$ icosahedral lattice. Further details of the morphology and RNA/protein composition of CCMV are given elsewhere (Bancroft & Flack, 1972; Kaper, 1975).

Studies of the assembly and dissociation of CCMV in vitro (Jacrot, 1975; Verduin, 1974, 1978; Adolph & Butler, 1974) indicate the following. Stable virus particles, sedimenting at 88 S, are obtained at pH 5. Increasing the pH to 7.5 increases the hydrodynamic volume of the virion, thus lowering the sedimentation value (78 S). In the presence of Mg^{2+} (Bancroft, 1970), partially swollen virus of sedimentation value 85 S is obtained. The completely swollen virion is susceptible to the action of both ribonuclease and protease (Bancroft et al., 1968). It has been proposed (Jacrot, 1975) that swelling is mediated by electrostatic repulsion between protein carboxyl groups that titrate at abnormally high pH. Spectrophotometric (Adolph, 1975) and NMR spectroscopic results (Vriend et al., 1982a) confirm structure changes in the coat subunit but do not indicate any significant change in RNA conformation with pH-induced swelling of the virion.

Increasing the solution ionic strength ($I > 1.0$) at pH 7.5 dissociates the swollen virus into free RNA and subunit dimers. At acidic pH, the subunit dimers reassociate into capsidlike shells, previously designated "pseudo-top components" (Bancroft et al., 1968) and here referred to as "capsids". These reconstituted capsids do not contain RNA.

Tryptic digestion of the subunit dimer excises a 25-residue segment from each N-terminus (Agrawal & Tremaine, 1972; Chidlow & Tremaine, 1971). The resulting core-protein dimers are stable at pH 7 and retain the ability to reassemble into "core capsids". NMR studies of virus, capsid, and core capsid (Vriend et al., 1981, 1982b) show that it is the N-terminal segment that undergoes a change in mobility upon interaction with RNA. The N-terminus may therefore play a role in binding RNA within the virion. Conversion of the N-terminus from a flexible coil to a more rigid α-helical conformation has been considered consistent with the NMR data (Vriend et al., 1982b).

In the present study, we employ laser Raman spectroscopy to investigate structures of CCMV and to detect conformational changes of CCMV RNA and coat protein as a function of solution pH and ionic strength. The rationale for application of the Raman effect to virus structure studies has been detailed previously (Thomas, 1976). We also employ Raman difference spectroscopy to detect subtle spectral changes indicative of amino acid and nucleotide residue interactions in the nucleoprotein particles (Thomas et al., 1983). To assist in the interpretation of data from CCMV, spectra have been obtained on CCMV components, including protein-free RNA and subunit and core subunit molecules in the capsid and dimeric states of assembly.

The present results permit us to draw conclusions about the protein–protein and protein–RNA interactions of the virion at different stages of the in vitro assembly pathway. Secondary structures of viral RNA and protein components are also inferred from the Raman spectra. These features of CCMV structure are compared with parallel results obtained previously

† From the Department of Virology, Agricultural University, 6709 PD Wageningen, The Netherlands (B.J.M.V.), and the Department of Chemistry, Southeastern Massachusetts University, North Dartmouth, Massachusetts 02747 (B.P. and G.J.T.). *Received January 24, 1984.* This is paper 12 in the series "Studies of Virus Structure by Laser Raman Spectroscopy". Paper 11 in this series is Thomas et al. (1983). This work was supported by NIH Grant AI11855.

0006-2960/84/0423-4301$01.50/0

on other RNA plant and bacterial viruses.

Experimental Procedures

CCMV was grown and purified as described previously (Verduin, 1978). Viral protein was isolated by the $CaCl_2$ method (Verduin, 1974). Core protein lacking the N-terminal region was prepared by trypsin digestion of subunit dimers at pH 7.5 (Chidlow & Tremaine, 1971; Tremaine et al., 1972). Viral protein in 300 mM NaCl plus 50 mM tris(hydroxymethyl)aminomethane hydrochloride (Tris-HCl) at pH 7.5 was mixed with ENZITE agarose–trypsin (E/S = 1/100) and incubated for 12 h at 4 °C with continuous stirring. The agarose–trypsin was removed by low-speed centrifugation, and low molecular weight cleavage products were removed by dialysis against 1.0 M NaCl plus 50 mM $NaC_2H_3O_2$, buffered at pH 5.0. Capsids and core capsids were obtained by dialysis of the appropriate protein against 1.0 M NaCl at pH 5.0. Protein-free RNA was obtained by phenol extraction of the virus (Verduin, 1978).

CCMV preparations were dialyzed for 24 h against 0.3 M NaCl, 10 mM $MgCl_2$, and 10 mM Tris-HCl at pH 5.0 or 7.6 ± 0.1, depending upon whether native or swollen particles, respectively, were being prepared. The dialyzate was then subjected to a low-speed spin (5000 rpm) for 0.25 h to remove debris, followed by a high-speed spin (40000 rpm) for 4 h to pellet the nucleoprotein. The pellets generally contained a nucleoprotein concentration of 70 ± 10 mg/mL as determined by the absorbance at 260 nm. All virus preparations were maintained at 4 °C throughout isolation and purification procedures. Electron micrographs of negatively stained particles confirmed no substantial loss of viral RNA.

Similar protocols were used to prepare capsids (pH 5.0 buffer) and dimers (pH 7.5 buffer) for Raman spectroscopy. Capsids were pelleted at ca. 70 mg/mL, and dimers were concentrated to the same density in an Amicon concentrator. Identical procedures were employed for both the native and core-protein subunits.

The phenol-extracted RNA solution, containing approximately 1 mg of RNA/mL of buffer (0.3 M NaCl + 10 mM $MgCl_2$ + 10 mM Tris-HCl), was ethanol precipitated to yield a pellet of RNA that was rinsed with 90% ethanol and lightly dried. The RNA was redissolved to 35 mg/mL in the same buffer at three different pH values: 3.6, 5.0, and 7.5.

Aliquots of 10 μL of each of the above virus, protein, and RNA solutions were sealed in Raman capillary cells (Kimax 34507), and each was thermostated at 8 ± 0.5 °C in the spectrometer (Thomas & Barylski, 1970). Spectra were excited with 300 mW of 514.5-nm radiation from an argon laser (Spectra Physics Model 171-18) and were recorded on a Spex Ramalog VI spectrometer under the control of a North Star Horizon II microcomputer (Li et al., 1981). The spectra shown below were obtained with a spectral slit width of 8 cm^{-1} and are the computer average of multiple scans as indicated in the figure legends. Generally, five scans were averaged for the region 300–1800 cm^{-1} and 25 scans for the region 2500–2600 cm^{-1}. Each component in the average was also examined separately. Photon counts were taken at increments of 1 cm^{-1} with an integration time of 1 s. All averaged spectra were corrected for solvent background by subtraction of the spectrum of the appropriate buffer. Spectra of CCMV and some protein samples also required correction for a slightly sloping background, which resulted from sample fluorescence.

All Raman intensities are reproducible to ±5%. In difference spectra, only those peaks that exceed the noise level by a factor of 2 or greater are considered significant. For each difference spectrum shown, the ordinate (number of photon counts) is scaled equal to that of the topmost spectrum in the same figure.

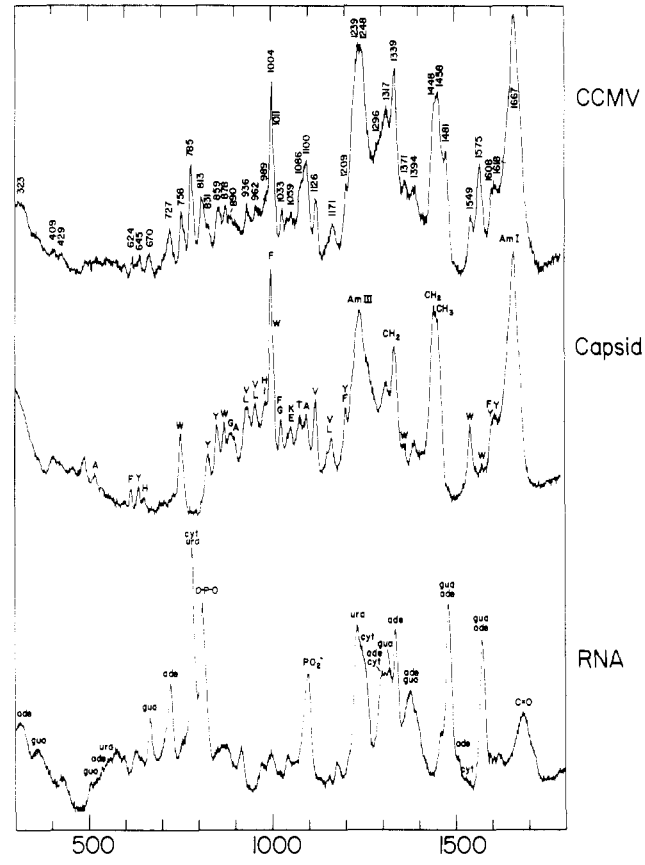

FIGURE 1: Raman spectra in the region 300–1800 cm^{-1} of native virus (70 mg/mL), capsid (70 mg/mL), and RNA (30 mg/mL) of CCMV, each at 8 °C and pH 5.0 in 0.3 M NaCl + 10 mM $MgCl_2$ + 10 mM Tris-HCl. Each spectrum shown is the average of five scans, corrected for solvent background. Other conditions are given in the text.

Results and Discussion

(1) Raman Assignments and Macromolecular Secondary Structures. Raman spectra in the region 300–1800 cm^{-1} of the CCMV virion, capsid, and RNA, each at pH 5, are shown in Figure 1. All prominent Raman lines in the spectra are assigned to RNA or protein groups as indicated in Figure 1 and summarized in Table I. The rationale for assignments is similar to that employed previously with other ribonucleoprotein particles (Thomas, 1976; Hartman et al., 1978; Fish et al., 1981; Thomas et al., 1980, 1976). The relative intensities of Raman lines of protein and RNA in the virus spectrum are consistent with their 76:24 weight percent ratio. A cursory examination of the data of Figure 1 also indicates that the virus spectrum is nearly, but not exactly, the sum of the spectra of its capsid and RNA constituents. The subtle spectral changes that do occur upon combining RNA and protein into virion are revealed by Raman difference spectroscopy, and their structural significance will be discussed (sections 2–8).

The characteristic Raman lines of the cysteinyl SH groups of capsid and virion subunits occur in the 2500–2600-cm^{-1} spectral range, displayed in Figure 2.

The Figure 1 spectrum of the capsid shows the amide I and amide III bands centered at 1666 and 1246 cm^{-1}, respectively, which indicates that the predominant secondary structure of the subunit is β-sheet (Chen & Lord, 1974; Lippert et al., 1976; Williams & Dunker, 1981). Weak shoulders to the main amide III band indicate additional β-conformation (1236

Table I: Raman Frequencies, Relative Intensities[a] and Assignments[b] of CCMV, CCMV Capsids, and CCMV RNA

CCMV	CCMV capsids	CCMV RNA	assignments	CCMV	CCMV capsids	CCMV RNA	assignments
323 (1.1 br)		320 (1.9)	Ade	1011 (6.1 sh)	1010 (6.2 sh)		W
368 (0.5)		363 (1.7)	Gua	1033 (2.1)	1029 (1.8)	1023 (0.7)	F, G; r
409 (0.7	407 (1.0)	392 (1.0)	skeletal; r	1046 (1.7)	1047 (1.1)	1044 (2.1)	r
429 (0.9)	428 (0.6)	430 (1.9)	skeletal; r	1059 (2.3)	1056 (1.7)	1063 (0.6)	K, E; r
	460 (0.5)		skeletal	1086 (4.7)	1081 (2.6)		T
497 (1.0)	493 (1.4)		skeletal	1100 (6.7)	1100 (2.9)	1099 (10.0)	A; PO_2^- str
		508 (2.2)	Gua	1126 (4.2)	1125 (3.9)		V (CC str)
525 (1.2)	522 (0.8)		skeletal, A	1158 (1.1)	1157 (1.1)	1158 (1.1)	V, L (CH_3 asym rock, ip); r
	541 (0.4)	536 (3.0)	skeletal; Ade	1171 (2.3)	1169 (1.9)	1179 (1.8)	V, L (CH_3 asym rock, op); r
556 (1.2)		559 (3.3)	Ura	1209 (4.6)	1207 (3.5)		F, Y
583 (1.1)		580 (3.6)	r		1226 (5.7 sh)		amide III
603 (1.0)	602 (0.4)	599 (2.4)	G; r	1239 (14.5)	1236 (7.9 sh)	1235 (15.4)	amide III; Ura
624 (1.2)	620 (1.2)		F	1249 (14.5)	1246 (8.9)	1247 (13.2)	amide III; Cyt
		633 (2.1)	r		1266 (6.0 sh)		amide III, H, Y
645 (1.6)	641 (1.3)	648 (1.1)	Y; r		1281 (4.4 sh)		amide III, H
	657 (0.8)		H	1296 (7.2 sh)		1300 (10.6)	Ade, Cyt
670 (1.7)		670 (4.8)	Gua	1317 (9.5)	1316 (4.9)	1319 (11.1)	CH_2 twist/wag, C–H def; Gua
710 (1.2 sh)	704 (0.6 br)	710 (3.1)	M; r	1339 (12.1)	1340 (6.8)	1338 (15.1)	CH_2 twist/wag; Ade
727 (2.9)		724 (7.7)	Ade	1371 (3.5)	1368 (1.2)	1377 (8.7)	W; Ade, Gua
737 (1.1 sh)	736 (1.2)		?	1394 (3.0)	1393 (1.5)	1391 (6.6)	CH_3 sym def; r
758 (3.8)	756 (4.5)	759 (2.0)	W; r	1417 (0.6)	1415 (1.2)	1416 (1.8)	CH_2 scissor (G), E; r
766 (2.2 sh)	763 (2.9 sh)		W	1448 (10.0 sh)	1448 (10.0)		CH_2 scissor
785 (6.9)		782 (21.8)	Cyt, Ura	1458 (11.0)	1458 (9.4 sh)	1460 (4.7)	CH_3 asym def, CH_2 scissor; r
813 (4.1)		812 (15.7)	O–P–O str	1481 (7.5)		1482 (18.2)	Gua, Ade
831 (1.8)	830 (2.7)		Y			1508 (2.7)	Ade
859 (2.6)	853 (3.8)	852 (1.5)	Y; r			1529 (1.0)	Cyt
878 (2.6)	874 (3.4)	870 (2.4)	W; r	1549 (4.3)	1548 (4.0)		W
890 (1.7)	892 (2.3)		G	1575 (8.0)	1582 (1.7)	1573 (15.1)	W; Gua, Ade
908 (1.0)	903 (1.8 sh)	916 (3.6)	A; r	1608 (6.2)	1606 (4.1)		F, Y
936 (2.0)	936 (2.9)		V, L (CH_3 sym rock, ip)	1618 (6.4) 1667 (19.1)	1617 (4.4) 1666 (13.4)	1621 (3.4)	Y amide I
962 (2.1)	960 (3.0)		V, L (CH_3 sym rock, op)			1683 (7.2) 1715 (3.0)	Ura (C=O str) Gua (C=O str)
		972 (2.5)	r	2551 (br)	2552 (br)		S–H str
989 (3.0)	986 (2.9)		H, I	2571	2571		S–H str
1004 (11.4)	1003 (10.2)	996 (3.4)	F; r				

[a] Intensities are relative to an arbitrary value of 10.0 for the 1448-cm^{-1} line of the capsid subunit or the 1099-cm^{-1} line of the RNA phosphate group, as appropriate. br = broad band; sh = shoulder. [b] When both protein and RNA residues contribute to the Raman line, their assignments are given to the left and right, respectively, of the semicolon. One- and three-letter symbols are employed, respectively, for amino acid and RNA-base residues. Standard chemical notation is used for phosphate, sulfhydryl, and hydrocarbon groups. Specific modes of CH_3 and CH_2 groups are designated as asymmetric (asym) or symmetric (sym) and as in-phase (ip) or out-of-phase (op), according to standard notation. Other abbreviations: str = stretching; def = deformation; r = ribose phosphate. See also Thomas et al. (1983).

cm^{-1}), as well as irregular (1266 cm^{-1}) and α-helix (1284 cm^{-1}) domains. Comparison of these data with results obtained on proteins of known secondary structure (Williams & Dunker, 1981; Pezolet et al., 1976) suggests 40–60% β-sheet and roughly 20–30% each of α-helix and irregular domains.

The well-characterized tyrosine doublet (Siamwiza et al., 1975) occurs in the capsid at 853 and 830 cm^{-1} with a peak intensity ratio of $I_{853}/I_{830} = 1.38 \pm 0.10$, which does not vary significantly for different states of the virion or capsid. Because there are five tyrosyl residues per subunit contributing to the observed doublet, no firm conclusions regarding individual tyrosine residues (Y-49, Y-137, Y-156, Y-158, and Y-189) are possible. However, if it is assumed that all tyrosines contribute equally to the doublet intensity, then the present results would be consistent with moderate hydrogen bonding of each *p*-hydroxyl group as both donor and acceptor of H bonds. This is the situation expected for tyrosyl side chains in contact with aqueous solvent (Siamwiza et al., 1975). The observed doublet could also arise from equal numbers of strong donor and strong acceptor OH groups. We find this unlikely, however, in view of the relative invariance of the intensity ratio to changes in pH and ionic strength and to proteolytic digestion of the N-terminal fragment (see below).

The three tryptophan residues per subunit (W-46, W-54, and W-93) are also presumed to exist in hydrophilic environments by virtue of their characteristic Raman lines near 760, 874, 1368, and 1548 cm^{-1} (Yu, 1974; Kitagawa et al., 1979; Thomas et al., 1983). This is consistent with the fluorescence data obtained by Krüse and co-workers (Krüse et al., 1979).

The hydrogen-bonding environment of cysteinyl SH groups in proteins has been studied previously by Alben and co-workers with Fourier-transform infrared spectroscopy (Alben et al., 1974). The appearance of two distinct SH stretching frequencies in the Raman spectra of Figure 2 confirms two different types of cysteinyl side chain environment in the subunits. The weak and broad band of lower frequency (2551 $\pm$ 2 cm^{-1}) indicates one class of SH group involved in hydrogen bonding with strong acceptors, e.g., H_2O, C=O, etc.; the sharp and higher frequency band (2571 cm^{-1}) indicates non-hydrogen-bonded or very weakly hydrogen-bonded SH groups, evidently shielded from solvent and other potential H-bond acceptors (Bare et al., 1975). The present results do not permit us to distinguish between C-58 or C-107 as the shielded cysteine residue.

The Figure 1 spectrum of CCMV RNA is characteristic of a highly ordered secondary structure, like that observed for other aqueous single-stranded RNA molecules. The Raman intensity ratio I_{812}/I_{1099} has the value 1.57 $\pm$ 0.03, which indicates that between 94 and 97% of nucleotide residues exist in paired or stacked configurations (Thomas & Hartman, 1973). Also evident from Figure 1 is the fact that no sig-

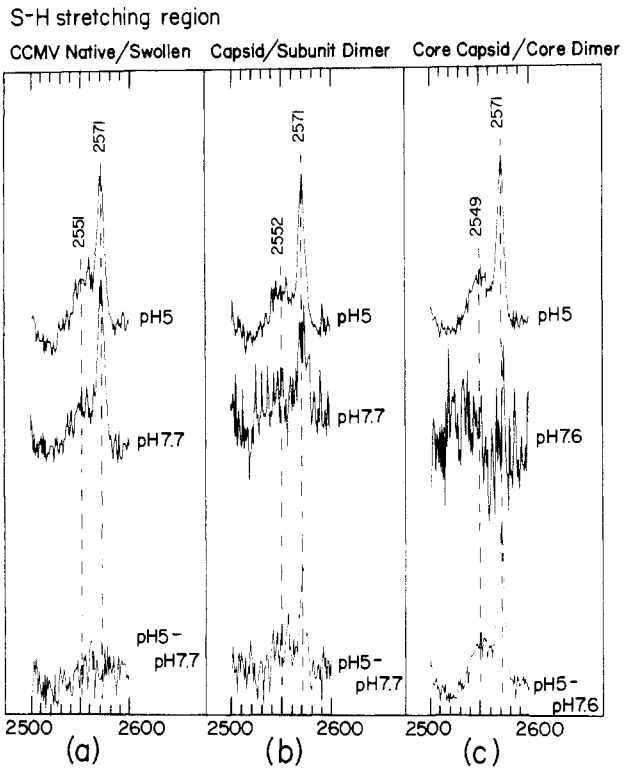

FIGURE 2: Raman spectra in the region 2500–2600 cm^{-1} of (a) native virus (pH 5.0) and swollen virus (pH 7.7) and their computed difference spectrum, (b) capsid (pH 5.0) and subunit dimer (pH 7.7) and their computed difference spectrum, and (c) core capsid (pH 5.0) and core dimer (pH 7.6) and their computed difference spectrum. Each spectrum shown is the average of 25 scans. Other conditions are as given in Figure 1.

nificant protonation of cytosine or adenine rings occurs at pH 5 in the *protein-free* CCMV RNA molecule (Hartman et al., 1978).

(*2*) *Subunit Structures in the Virion and Capsid Are Different.* Figure 3 shows the observed Raman spectrum of the capsid (top), a computed capsid spectrum (middle) generated by subtraction of the spectrum of CCMV RNA from that of virus, and a difference spectrum (bottom) obtained by subtraction of the computed capsid spectrum from the observed capsid spectrum. Thus, the observed and computed capsid spectra are not identical, and the computed differences (i.e., positive and negative bands in the difference spectrum of Figure 3) are diagnostic of the molecular subgroups that differ in the virion and capsid states. We find positive protein bands (assignments in parentheses) at 757 (W), 1004 (F), 1129 (CC stretching of aliphatic side chains), and 1344 cm^{-1} (CH_2 wagging), due to their higher Raman intensity in the capsid. Negative protein bands occur at 1228 (amide III), 1331 (CH_2 wagging) and 1662 cm^{-1} (amide I), due to higher Raman intensity in the virion. Negative RNA bands are also observed at 782 (Cyt + Ura), 1481 (Ade + Gua), and 1573 cm^{-1} (Ade + Gua). These shall be discussed in section 3.

Our interpretation of these results is the following. The environment of aromatic rings of tryptophan and phenylalanine residues is different in the virion and capsid states. The lower intensities at 757 and 1004 cm^{-1} in the virus, as compared with the capsid, suggest greater Raman hypochromism (Small & Peticolas, 1971) in the virion, possibly due to mutual stacking interactions of F and W residues of the subunits or to stacking with bases of the encapsidated RNA molecule. The 1228- and 1662-cm^{-1} lines indicate a change of subunit secondary structure with release of RNA from the virion. The positions of the amide bands are consistent with a loss of β-structure

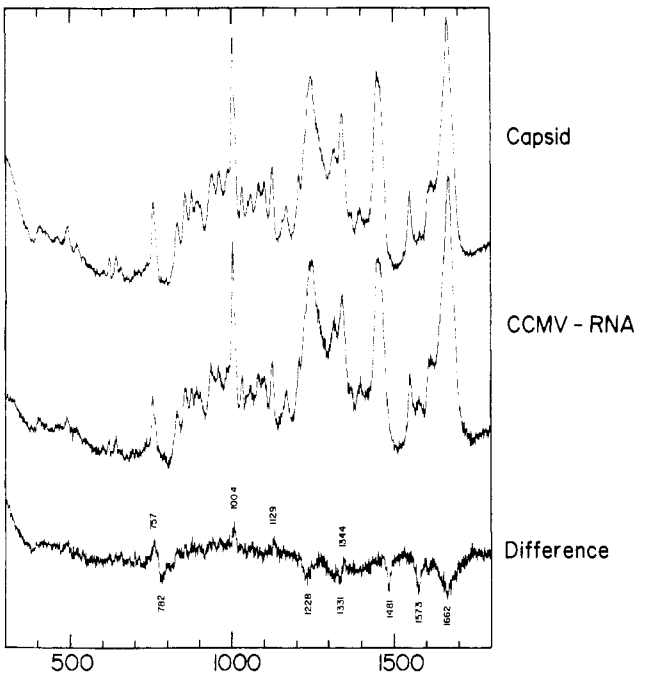

FIGURE 3: (Top) Observed spectrum of capsid. (Middle) Computed spectrum of capsid (observed spectrum of virus minus observed spectrum of RNA). (Bottom) Computed difference spectrum (top minus middle). Other conditions are as given in Figure 1.

accompanying the release of RNA. The magnitude of the amide III intensity change corresponds to about 5–10% more β-structure per subunit of the virion (Pezolet et al., 1976). Accordingly, the relative maximum near 1273 cm^{-1} in the difference spectrum of Figure 3 suggests conversion to α-helix. We note, however, that the difference spectrum of Figure 3 is not sufficiently noise-free to indicate conclusively whether the loss of β-structure in the capsid is accompanied by a concomitant gain of α-helix or other chain configuration. Finally, the intensity gain at 1129 cm^{-1} and the apparent shift of Raman intensity from 1331 to 1344 cm^{-1} with release of RNA are indications that aliphatic amino acid side chain configurations and/or environments are also altered by the change in state from virion to capsid. Similar Raman intensity changes are observed with salt-induced structure transitions in filamentous viruses and are attributable to disordering of aliphatic side chains (Thomas et al., 1983).

(*3*) *Encapsidated and Protein-Free RNA Molecules Are Structurally Different.* Figure 4 shows the spectrum observed for aqueous CCMV RNA after extraction from the virion (top), as well as a computed RNA spectrum (middle) generated by subtraction of the capsid spectrum from that of the virus. Also shown in Figure 4 is a difference spectrum (bottom), which is obtained by subtracting the computed RNA spectrum from the observed RNA spectrum. As expected, the difference spectrum of Figure 4 shows a close correspondence to the difference spectrum of Figure 3: Each represents the spectral differences between virion and the sum of its RNA and protein constituents. The virtual identity of the difference spectra of Figure 3 and 4 provides independent confirmation of the reliability of the computer subtraction routines employed for manipulation of Raman spectra of virus, capsid, and protein.

We find that the purine lines at 1483 and 1572 cm^{-1} are more intense in the encapsidated RNA molecule than in the protein-free RNA molecule. The intensity differences are small (approximately 5%) but significant and suggest that the purines are affected by the protein shell. The most reasonable

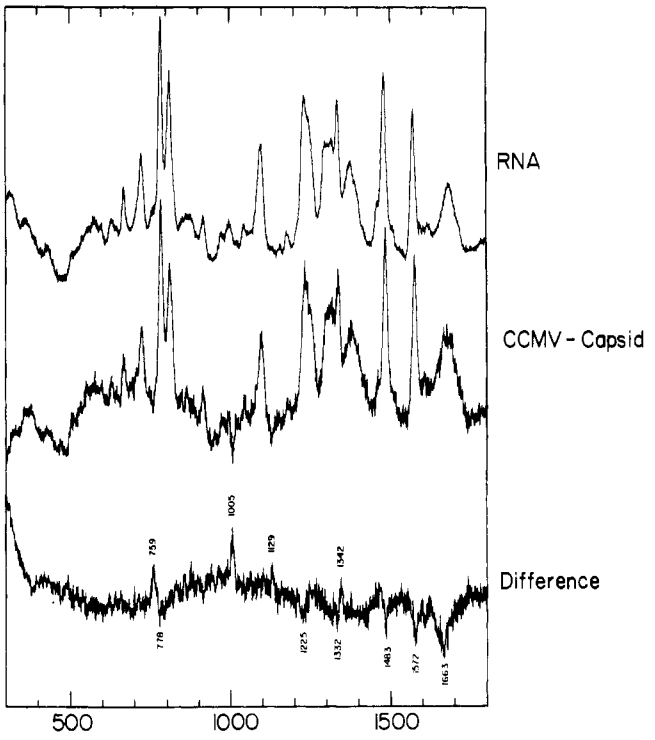

FIGURE 4: (Top) Observed spectrum of RNA. (Middle) Computed spectrum of RNA (observed spectrum of virus minus observed spectrum of capsid). (Bottom) Computed difference spectrum (top minus middle). Other conditions are as given in Figure 1.

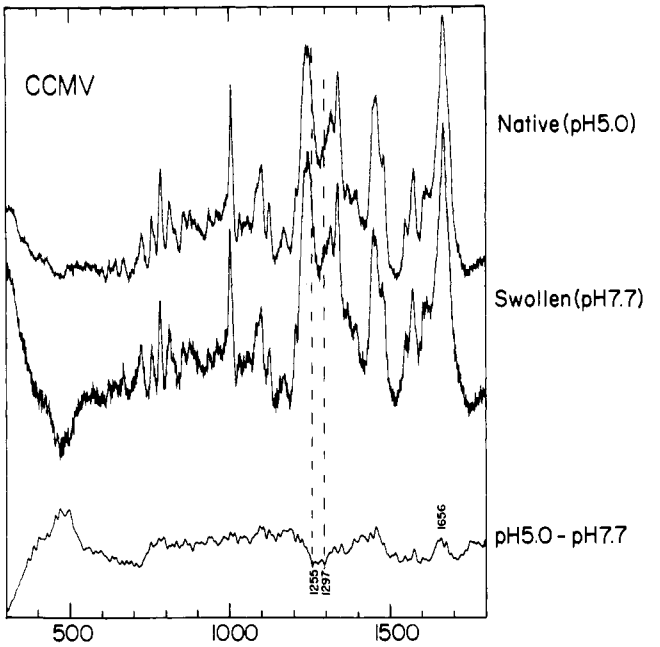

FIGURE 5: (Top) Observed spectrum of native virus, pH 5.0. (Middle) Observed spectrum of swollen virus, pH 7.7. (Bottom) Computed difference spectrum (top minus middle). Only bands of signal-to-noise ratio greater than 2:1 are labeled, as discussed in the text. Other conditions are as given in Figure 1.

interpretation of these data is that there occurs a reduction in purine–purine base stacking upon encapsidation of the RNA. The negative peak near 782 cm^{-1} in Figure 3 is barely evident in Figure 4, and its significance is somewhat in doubt. However, the apparent small shift of Raman intensity from just above to just below 800 cm^{-1} with encapsidation of RNA, as is indicated in Figure 3, is consistent with about 2% more order of the backbone of extraviral RNA. Therefore, the Raman data are consistent in indicating a slightly more ordered RNA secondary structure accompanying release from the virion.

(*4*) *Carboxyl Groups Do Not Titrate with Swelling of the Virion.* Figure 5 shows the Raman spectra of CCMV in native (pH 5.0) and swollen (pH 7.7) states and their difference spectrum. The high noise level in the original difference spectrum has been slightly attenuated by smoothing. The data show that only a few Raman lines are significantly affected by pH-induced swelling of the virion. It is also clear from the difference spectrum of Figure 5 that no negative peak occurs near 1400–1420 cm^{-1} ($-CO_2^-$ groups) and no positive peak occurs near 1700–1750 cm^{-1} (–COOH groups) as would be expected if carboxyl groups were titrated with increasing pH. We may conclude that titration of –COOH groups of aspartic and glutamic acid side chains does not occur over this pH range, a result that could be due in part to the presence of Mg^{2+} ions (Pfeiffer & Durham, 1977).

(*5*) *Subunit Secondary Structure Is Altered by Virion Swelling and RNA Bases May Be Deprotonated with the Accompanying Increase in pH.* Caution must be exercised in interpreting the relatively intense negative bands that are distinguished at 1255 and 1297 cm^{-1} in the difference spectrum of Figure 5. The trough at 1255 cm^{-1} (amide III) indicates a more disordered subunit secondary structure at pH 7.7 than at pH 5.0. This is consistent with the contour in the amide I region, which suggests that the disordering at pH 7.7 occurs at the expense of α-helix. Since nonidentical base lines in the constituent spectra and overlapping cytosine lines (below) may also affect the intensity of the 1255-cm^{-1} difference trough, a quantitative estimate of the extent of secondary structure change is not warranted by these data.

The negative peak at 1297 cm^{-1} is assigned to RNA groups and is consistent with the conversion of a small percentage of RNA adenines from protonated to deprotonated states with increasing pH (see section 8). We note also that deprotonation of cytosines should cause a positive intensity change near 1263 cm^{-1} (Chou & Thomas, 1977; Hartman et al., 1978). However, such a feature in the difference spectrum is apparently more than compensated by the observed amide III change at nearly the same frequency.

From Figure 2, we note that the pattern of SH stretching frequencies is unchanged by swelling of the virion. Therefore, the environments of the two classes of cysteinyl side chains do not change significantly with swelling.

(*6*) *Dissociation of Capsids Does Not Alter Subunit Secondary Structure but Affects the Environment of Amino Acid Side Chains.* Figure 6 shows spectra of the CCMV capsid at pH 5.0 and 7.7 and its corresponding difference spectrum. No significant change in subunit secondary structure is evident from the difference spectrum. The peaks at 896 and 1098 cm^{-1} and the troughs at 816, 1061, and 1121 cm^{-1} are all due to aliphatic amino acid side chains (Thomas et al., 1983). Therefore, although the environment of these side chains is altered with capsid disassembly, there is no accompanying net change in the overall secondary structure of the subunits.

Figure 2 confirms also a change in the environment of cysteinyl SH groups with capsid disassembly. We detect a 50% reduction in the peak intensity of the 2571-cm^{-1} line, indicating that half of the solvent-shielded class of SH groups is affected. The signal-to-noise ratio does not permit us to conclude whether such groups are converted to the hydrogen-bonded class, i.e., whether a concomitant Raman intensity increase occurs in the broad band near 2551 cm^{-1}, or whether the SH groups are chemically modified, e.g., converted to disulfides. If cystine bridges were formed between subunits in the dimeric state, we would expect a detectable Raman line

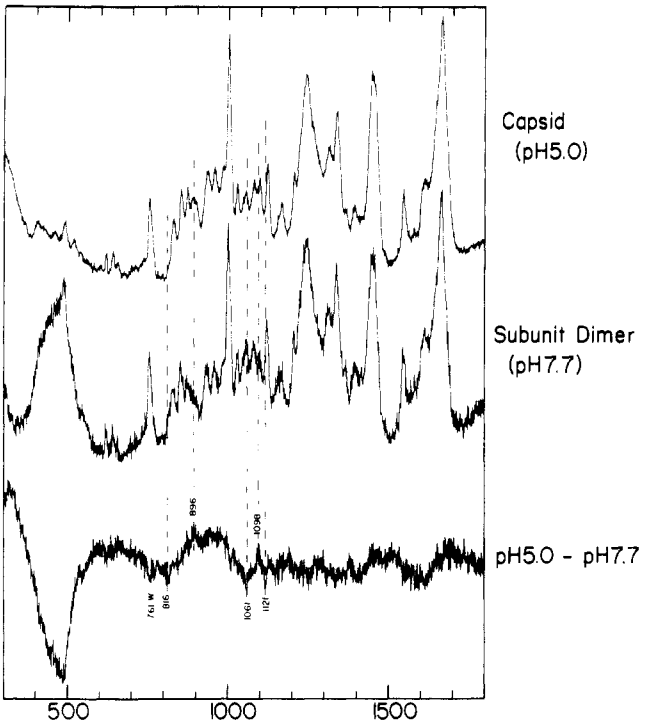

FIGURE 6: (Top) Observed spectrum of capsid in 0.3 M NaCl + 10 mM $MgCl_2$ + 10 mM Tris-HCl, pH 5.0. (Middle) Observed spectrum of subunit dimer in 0.3 M NaCl + 10 mM $MgCl_2$ + 10 mM Tris-HCl, pH 7.7. (Bottom) Computed difference spectrum (top minus middle). Other conditions are as given in Figure 1.

near 490–525 cm^{-1} from the characteristic SS stretching frequency (Lord & Yu, 1970). As seen in Figure 6, the background of solvent interference is rather severe in the 300–550-cm^{-1} interval, making difficult the detection of a putative SS Raman line. Further study of this question must await the availability and investigation of more concentrated preparations of the capsid and subunit dimers.

(7) *Core Capsid Disassembly Yields Complex Protein Structure Changes.* Figures 2 and 7 show that the effects of pH-induced disassembly of core capsids are more pronounced and more complex than those observed for capsids. In the absence of better characterization of the core-protein assembly states, detailed discussion of these results is not warranted. However, the data do confirm here, as above, the sensitivity of aliphatic amino acid side chains to the pH-induced disassembly. Particularly striking is the effect upon the SH stretching region (Figure 2), where both the sharp 2571-cm^{-1} line and the broad 2549-cm^{-1} line are greatly attenuated at neutral pH. The resulting very weak and broad profile of Raman scattering, barely detectable over the background noise, is evidently due to the presence of a broad spectrum of hydrogen-bonded SH groups in core dimer preparations. Since an intense Raman line may be present in the SS region, it is also possible that substantial oxidation of SH groups has occurred.

(8) *Protonated Bases Do Occur in Encapsidated RNA of the Virion at pH 5.* Figure 8 shows Raman spectra of purified (protein-free) CCMV RNA at three different pH values: 7.5, 5.0, and 3.6. Also shown are difference spectra between pH values 5.0 and 7.5 and between 3.6 and 7.5. All of the Raman peaks and troughs in the difference spectrum (pH 3.6 minus pH 7.5) can be attributed respectively to increased concentrations of protonated bases (mainly Ade^+ and Cyt^+, but also Gua^+) and decreased concentrations of nonprotonated bases at the lower pH (Lord & Thomas, 1967a), except for the peak at 795 cm^{-1} and the trough at 812 cm^{-1}, which are both due

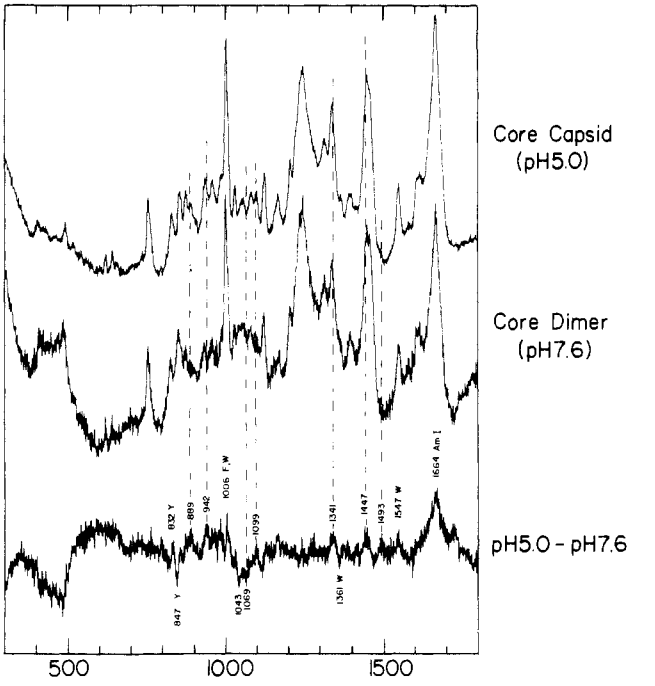

FIGURE 7: (Top) Observed spectrum of core capsid in 0.3 M NaCl + 10 mM $MgCl_2$ + 10 mM Tris-HCl, pH 5.0. (Middle) Observed spectrum of core dimer in 0.3 M NaCl + 10 mM $MgCl_2$ + 10 mM Tris-HCl, pH 7.6. (Bottom) Computed difference spectrum (top minus middle). Other conditions are as given in Figure 1.

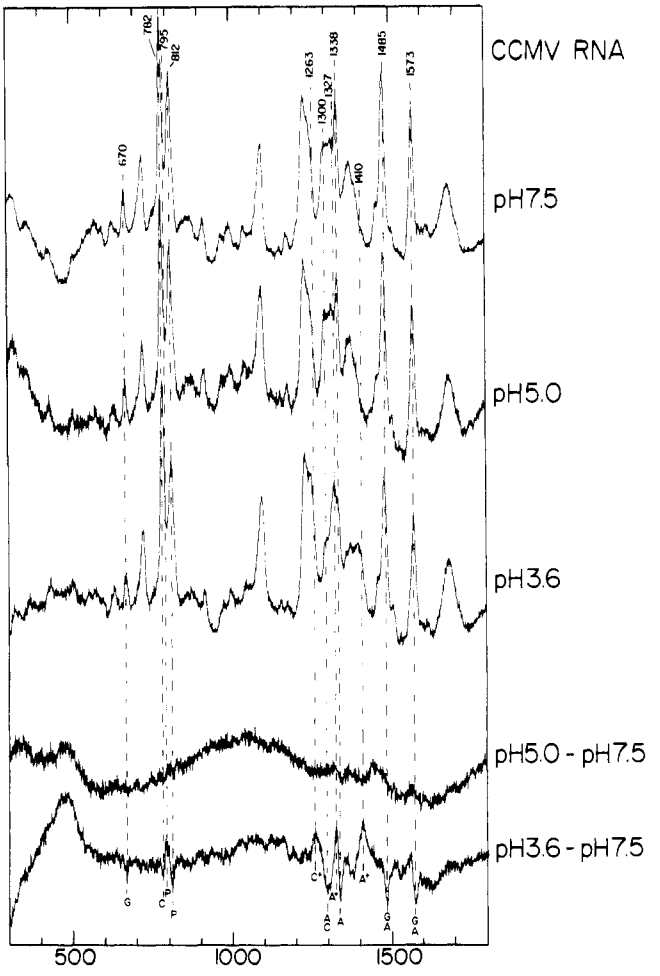

FIGURE 8: Raman spectra of protein-free CCMV RNA in 0.3 M NaCl + 10 mM $MgCl_2$ + 10 mM Tris-HCl: (from top to bottom) observed, pH 7.5; observed, pH 5.0; observed, pH 3.6; computed difference, pH 5.0 minus 7.5; computed difference, pH 3.6 minus 7.5. Other conditions are as given in Figure 1.

to the greater secondary structure of RNA near neutral pH (Thomas & Hartman, 1973). As shown previously, the extent of both base protonations (Lord & Thomas, 1967b) and secondary structure (Thomas & Hartman, 1973) can be quantified by measurement of the appropriate Raman line intensities. The difference spectra of Figure 8 thus show that less than 5% of Ade and less than 3% of Cyt residues are protonated and that less than 3% of the ordered secondary structure of RNA is lost with reduction of the pH from 7.5 to 5.0, whereas 7% of Cyt and 15% of Ade residues are protonated and 10% of the ordered RNA structure is lost with reduction of the pH to 3.6.

Comparison of the difference spectra of Figure 8 with the difference spectrum of Figure 5 indicates that Ade and Cyt residues of encapsidated CCMV RNA are more protonated at pH 5 than are corresponding bases of naked RNA at the same pH value. We find that all relative peaks and troughs correspond closely in the two difference spectra, excepting amide I and III features for reasons discussed above (section 5). We conclude from the observed peak intensities in the difference spectrum of Figure 5, and from the data of Figure 8 employed for calibration, that the limits of protonation of Cyt and Ade residues in encapsidated RNA are $3\% < Cyt^+ < 7\%$ and $5\% < Ade^+ < 15\%$, respectively. Further, we find no protonation of Gua rings in encapsidated RNA, even though significant Gua protonation occurs in protein-free RNA at pH 3.6.

Summary

The major conclusions of this work are the following. (i) Both RNA and protein subunits in the virion are highly ordered structures. The bases of the genome are predominantly paired and stacked, presumably in hairpin helices, and the backbone of encapsidated RNA contains the conventional C3′-endo or "A-RNA" geometry. The predominant secondary structure in the subunit of the virion is β-sheet. These features of macromolecular conformation are similar to those observed in MS2 and TYMV (Thomas et al., 1976; Hartman et al., 1978) and correlate well with the β-barrel models proposed for other RNA plant viruses (Harrison, 1983). (ii) Two spectroscopically different classes of cysteinyl SH groups are observed in the subunit of the native virion, swollen virion, and capsid. One class is characterized by relatively strong hydrogen bonding and the other by shielding from hydrogen bonding to negative acceptors. The latter (hydrophobic class) is progressively eliminated by dissociation of the capsid into dimers and by proteolytic digestion of the 25-residue segment of the N-terminus. (iii) Tyrosine side chains exist on average with the *p*-hydroxy groups in contact with hydrogen-bonding donor and acceptor groups for all subunit states (virion, capsid, and dimer) examined. (iv) Tryptophan and phenylalanine residues exhibit different environments in virion and capsid states, which suggests that these aromatics are directly involved in interaction with RNA. (v) Configurations of aliphatic amino acid side chains and secondary structure of the subunit main chain are also altered by release of RNA from the virion. Further, the secondary structure of encapsidated RNA is characterized by different base stacking and by a slightly less ordered backbone than occurs in protein-free RNA. (vi) Swelling of the virion by increasing the pH from 5.0 to 7.5 does not titrate aspartate or glutamate COOH groups but does titrate small numbers of Ade^+ and Cyt^+ residues of encapsidated RNA. (vii) The protonation of RNA bases in the virion at pH 5 is limited to adenines and cytosines. The following semiquantitative estimates of the percentages of protonated bases are deduced from the Raman intensity measurements: $3\% < Cyt^+ < 7\%$ and $5\% < Ade^+ < 15\%$. The protonated bases thus require both a capsid envelope and pH 5 for their stabilization, since no protonated bases are evident in the pH 7 (swollen) virion and fewer protonated bases are evident in naked RNA at pH 5.

The present results reveal a CCMV subunit secondary structure that is sensitive to swelling of the virion and to the release of the encapsidated RNA. In addition, the microenvironments of aliphatic and aromatic amino acid side chains are substantially altered by the same changes in assembly or morphological state of the capsid, as well as by dissociation of the capsid into dimers.

Models for CCMV structure should account for the occurrence of protonated pyrimidines (Cyt^+) and purines (Ade^+) in the native virion and the absence of protonated carboxyl groups of aspartic and glutamic acid side chains. The latter, as well as the C-terminus of the subunit main chain, can on the other hand provide negatively charged groups for electrostatic interaction with positively charged bases of the RNA genome. Such interactions would be eliminated by increasing the pH, which would also permit the RNA to assume a secondary structure more nearly like that of protein-free aqueous RNA. Also implicated in RNA–protein interaction in the virion are the tryptophan, phenylalanine, and aliphatic side chains of the subunit. The present results do not allow us to identify more specifically the interacting residues; however, additional investigations are in progress to identify by selective labeling the interacting tryptophan(s).

Attenuation of RNA–protein interactions by virion swelling, as well as by release of RNA from the capsid, profoundly alters the characteristic CC stretching and CH_2 deformation modes of the subunit side chains, similar to that observed in the conformational transitions of filamentous viruses (Thomas et al., 1983). The present results are certainly consistent with those of NMR studies of CCMV (Vriend et al., 1981, 1982a), which have yielded evidence for the influence of RNA upon the mobility of the basic N-terminus of the virion subunit. Further, it is precisely the CC and CH_2 characteristic Raman lines that would be most affected if lysyl and arginyl side chains were configured differently in the presence and absence of RNA binding by the basic N-terminus. Yet, it is important to recognize that the NMR and Raman transitions occur on greatly different time scales and do not necessarily indicate structural changes in the same protein domains. The present Raman results are just as likely to reflect altered protein–protein interactions accompanying swelling and dissociation of the capsids.

The model of CCMV that emerges from these studies is one in which RNA–protein interactions stabilize the ribonucleoprotein particle. The data are not inconsistent with the proposal of Rossmann and co-workers (Rossmann et al., 1983) that β-sheet domains of the subunits provide the sites for RNA binding.

Dissociation of the virion into RNA and capsid clearly alters the Raman intensities of characteristic vibrational modes of aromatic and aliphatic side chains and RNA bases. Electrostatic interactions between protonated base residues and protein subgroups are also diminished with virion swelling and result in the RNA molecule assuming a more aqueous-like environment within the protein shell. The β-rich subunits are versatile in their ability to undergo secondary structure changes and altered side-chain configurations with swelling, RNA release, disassembly, and N-terminal excision. Unexpectedly, the cysteinyl SH groups are significantly altered by disassembly of capsid and core-capsid aggregates into dimers but

are unaffected by capsid expansion.

Acknowledgments

We thank Professor Jonathan King of the Department of Biology, MIT, for use of electron microscope facilities and Erika Hertwieg for expert technical assistance in obtaining micrographs of CCMV preparations.

References

Adolph, K. W. (1975) *J. Gen. Virol. 28*, 137–145.
Adolph, K. W., & Butler, P. J. G. (1974) *J. Mol. Biol. 88*, 327–347.
Agrawal, H. O., & Tremaine, J. H. (1972) *Virology 47*, 8–20.
Alben, J. O., Bare, G. H., & Bromberg, P. A. (1974) *Nature (London) 252*, 736–739.
Bancroft, J. B. (1970) *Adv. Virus Res. 16*, 99–134.
Bancroft, J. B., & Flack, I. H. (1972) *J. Gen. Virol. 15*, 247–251.
Bancroft, J. B., Hiebert, E., Rees, M. W., & Markham, E. (1968) *Virology 34*, 224–239.
Bare, G. H., Alben, J. O., & Bromberg, P. A. (1975) *Biochemistry 14*, 1578–1588.
Chen, M. C., & Lord, R. C. (1974) *J. Am. Chem. Soc. 96*, 4750–4752.
Chidlow, J., & Tremaine, J. H. (1971) *Virology 43*, 267–278.
Chou, C. H., & Thomas, G. J., Jr. (1977) *Biopolymers 16*, 765–789.
Fish, S. R., Hartman, K. A., Stubbs, G. J., & Thomas, G. J., Jr. (1981) *Biochemistry 20*, 7449–7457.
Harrison, S. C. (1983) *Adv. Virus Res. 28*, 175–240.
Hartman, K. A., McDonald-Ordzie, P. E., Kaper, J. M., Prescott, B., & Thomas, G. J., Jr. (1978) *Biochemistry 17*, 2118–2123.
Jacrot, B. (1975) *J. Mol. Biol. 95*, 433–446.
Kaper, J. M. (1975) *The Chemical Basis of Virus Structure, Dissociation and Reassembly*, North-Holland, Amsterdam.
Kitagawa, T., Azuma, T., & Hamaguchi, K. (1979) *Biopolymers 18*, 451–465.
Kruse, J., Verduin, B. J. M., & Visser, A. J. W. G. (1979) *Eur. J. Biochem. 95*, 21–29.
Lane, L. C. (1974) *Adv. Virus Res. 19*, 151–220.
Li, Y., Thomas, G. J., Jr., Fuller, M., & King, J. (1981) *Prog. Clin. Biol. Res. 64*, 271–283.
Lippert, J. L., Tyminski, D., & Desmeules, P. J. (1976) *J. Am. Chem. Soc. 98*, 7075–7080.
Lord, R. C., & Thomas, G. J., Jr. (1967a) *Spectrochim. Acta, Part A 23A*, 2551–2591.
Lord, R. C., & Thomas, G. J., Jr. (1967b) *Biochim. Biophys. Acta 142*, 1–11.
Lord, R. C., & Yu, N.-T. (1970) *J. Mol. Biol. 50*, 509–524.
Pezolet, M., Pigeon-Gosselin, M., & Coulombe, L. (1976) *Biochim. Biophys. Acta 453*, 501–512.
Pfeiffer, P., & Durham, A. C. (1977) *Virology 81*, 419–432.
Rossmann, M. G., Abad-Zapatero, C., Erickson, J. W., & Savithri, H. S. (1983) *J. Biomol. Struct. Dynam. 1*, 565–579.
Siamwiza, M. N., Lord, R. C., Chen, M. C., Takamatsu, T., Harada, I., Matsuura, H., & Shimanouchi, T. (1975) *Biochemistry 14*, 4870–4876.
Small, E. W., & Peticolas, W. L. (1971) *Biopolymers 10*, 69–88.
Thomas, G. J., Jr. (1976) *Appl. Spectrosc. 30*, 483–494.
Thomas, G. J., Jr., & Barylski, J. (1970) *Appl. Spectrosc. 24*, 463–464.
Thomas, G. J., Jr., & Hartman, K. A. (1973) *Biochim. Biophys. Acta 312*, 311–322.
Thomas, G. J., Jr., Prescott, B., McDonald-Ordzie, P. E., & Hartman, K. A. (1976) *J. Mol. Biol. 102*, 103–124.
Thomas, G. J., Jr., Prescott, B., & Hamilton, M. G. (1980) *Biochemistry 19*, 3604–3613.
Thomas, G. J., Jr., Prescott, B., & Day, L. A. (1983) *J. Mol. Biol. 164*, 321–356.
Tremaine, J. H., Agrawal, H. O., & Chidlow, J. (1972) *Virology 48*, 245–254.
Verduin, B. J. M. (1974) *FEBS Lett. 45*, 50–54.
Verduin, B. J. M. (1978) *J. Gen. Virol. 39*, 131–147.
Vriend, G., Hemminga, M. A., Verduin, B. J. M., DeWit, J. L., & Schaafsma, T. J. (1981) *FEBS Lett. 134*, 167–171.
Vriend, G., Hemminga, M. A., Verduin, B. J. M., & Schaafsma, T. J. (1982a) *FEBS Lett. 146*, 319–321.
Vriend, G., Verduin, B. J. M., Hemminga, M. A., & Schaafsma, T. J. (1982b) *FEBS Lett. 145*, 49–52.
Williams, R. W., & Dunker, A. K. (1981) *J. Mol. Biol. 152*, 783–813.
Yu, N.-T. (1974) *J. Am. Chem. Soc. 96*, 4664–4668.